Carbohydrate Polymers 88 (2012) 154–164

Contents lists available at SciVerse ScienceDirect

Carbohydrate Polymers

journal homepage: www.elsevier.com/locate/carbpol

Introduction of various functionalities into polysaccharides using alkynyl ethers as precursors: Pentynyl dextrans

M. Nazir Tahir[a,1], Nico Lämmerhardt[a,b], Petra Mischnick[a,c,*]

[a] Technische Universität Braunschweig, Institute of Food Chemistry, Schleinitzstr. 20, D-38106 Braunschweig, Germany
[b] Technische Universität Braunschweig, Institute of Semiconductor Technology, Hans-Sommer-Str. 66, D-38106 Braunschweig, Germany
[c] Royal Institute of Technology, KTH Stockholm, Fibre and Polymer Technology, Tekninkringen 56-58, SE-10044 Stockholm, Sweden

ARTICLE INFO

Article history:
Received 21 September 2011
Received in revised form 5 November 2011
Accepted 24 November 2011
Available online 7 December 2011

Keywords:
Alkynyl dextran
Functionalized dextrans
Biotinyl dextran
Tocopheryl dextran
Click-chemistry

ABSTRACT

Following the concept of using *O*-alkynyl glycans as key precursors of functional polysaccharides, dextran derivatives with nearly the same distritbution pattern, but various functional groups – for common (bio)conjugation reactions, molecular recognition, and antioxidant activity – have been prepared. Pentynyl dextran well characterized with respect to the degree of substitution (DS 0.43) and the distribution of alkynyl groups to the various OH of the glucosyl unit, was further modified by 1,3-dipolar cycloaddition of various functionalized azides, thus introducing amino, hydroxy, thiol, and carboxyl groups with good to quantitative yield. Besides these functional groups, biotin and tocopherol were introduced with about 60% conversion of alkyne groups. Biotinylated dextran was demonstrated to bind specifically to fluorophor-labeled streptavidin, while glucose linked tocopherol did not show loss of antioxidant activity. Formation of triazole derivatives was proved by ATR-IR and NMR spectroscopy, and after methanolysis of the dextran, by ESI mass spectrometry. Degree of conversion was estimated from ^{1}H NMR spectra, decrease of pentynyl groups in the product mixture analyzed by GLC, and elemental analysis.

1. Introduction

Dextrans are α-1,6-linked glucans; they are randomly branched to different degrees at O-3, but in some cases also at O-4 and O-2, depending on the producing strain of *Leuconostoc mesenteroides*, e.g. to 5% at O-3 for *L. mesenteroides*. NRRL B-512F (Heinze, Liebert, Heublein, & Hornig, 2006). Chemical modification changes their properties and opens new fields of application for these biocompatible, non-toxic natural products. For example, amphiphilic dextrans (Durand, Marie, Rotureau, Leonard, & Dellacherie, 2004; Rotureau, Leonard, Dellacherie, & Durand, 2004) have been used for nanoparticle coating and as drug carrier systems in emulsion polymerization (Aumelas, Serrero, Durand, Dellacherie, & Leonard, 2007), or direct nanoparticle formation (Hornig & Heinze, 2007; Hornig, Heinze, Hesse, & Liebert, 2005; Hornig, Liebert, & Heinze, 2007; Liebert, Hornig, Hesse, & Heinze, 2005). We have used terminal-unsaturated ethers of glucose and amylose as key precursors for further functionalization in several model studies (Tahir et al., 2010; Tankam, Mischnick, Hopf, & Jones, 2007; Tankam, Müller, Mischnick, & Hopf, 2007). Alkynyl ethers of polysaccharides are interesting products themselves, but also as intermediates to introduce a number of additional functionalities at defined positions, since the distribution of the alkynyl groups can be determined precisely after the first derivatization step (Tahir et al., 2010). This is less simple for larger substituents or acid sensitive groups, since acid hydrolysis and gas chromatography in combination with mass spectrometry (GC/MS) are the most powerful methods for such differentiated quantitative analyses (Mischnick & Momcilovic, 2010), which is not possible by NMR spectroscopy. Thus, by this approach, polysaccharide derivatives with various functionalities, but identical substitution pattern, become available, since the latter is controlled in the first reaction step. Combining carbohydrate and acetylene chemistry links a hydrophilic polysaccharide to a rigid, hydrophobic functional group. Inter alia, the terminal C≡C triple bond can undergo 1,3-dipolar cycloaddition reactions with azides under mild conditions, a process that tolerates numerous other functional groups. Since the introduction of this Cu(I)-catalyzed variant of the Huisgen reaction to afford 1,2,3-triazoles as "click-chemistry" by Sharpless and co-workers (Kolb, Finn, & Sharpless, 2001) and Meldal et al. (Tornoe, Christensen, & Meldal, 2002), the use of alkynyl modified carbohydrates has drastically increased (Bock, Heimstra, & Maarseveen, 2006; Wilkinson, Bornaghi, Poulsen, & Houston, 2006). For example, "click-chemistry" has been applied to carbohydrate–alkynyl derivatives for the generation of synthetic receptors (Dorner & Westermann, 2005; Hasegawa et al., 2006) and for the visualization

* Corresponding author. Tel.: +49 531 3917201; fax: +49 531 3917230.
E-mail address: p.mischnick@tu-braunschweig.de (P. Mischnick).
[1] Present address: Laboratory of Organic Chemistry, Dreijenplein 8, Wageningen University, 6703 HB Wageningen, The Netherlands.

0144-8617/$ – see front matter © 2011 Elsevier Ltd. All rights reserved.
doi:10.1016/j.carbpol.2011.11.082

Nomenclature

ABTS	2,2-Azinobis-(3-ethylbenzothiazoline-6-sulfonic acid)
AGU	Anhydro glucose unit
DS	Degree of substitution
EA	Elemental analysis
ECR	Effective carbon response
EDC	1-Ethyl-3(3-dimethylaminopropyl)carbodiimide
NHS	*N*-Hydroxy succinimide
PyD	Pentynyl dextran
TEAC	Trolox equivalent antioxidant capacity

of glucoconjugates in cells (Hsu, Hanson, Kishikawa, Wang, Sawa, & Wong, 2007). In an interesting approach, biodegradable microcapsules have been produced by "clicking together" acetylenic and azido derivatives of dextrans, a method that has been further developed for degradable multilayer films and capsules (Geest, Camp, Prez, Smedt, Demeester, & Hennink, 2008) (Hennink, De Geest, Van Camp, & Du Prez, 2009). While in that case, it is advantageous to have the functional groups bound to the backbone by easily cleavable carbonate linkages, ethers allow further transformations under alkaline and acidic conditions and thus widen the range of possible follow-up reactions, making also use of the CH-acidity of terminal alkynes (Tankam, Mischnick et al., 2007). Most examples applying cycloaddition to triazoles have introduced azide functions by nucleophilic displacement of the modified primary 6-CH_2OH moiety of the polysaccharide backbone (Bertoldo, Nazzi, Zampano, & Ciardelli, 2011; Hasegawa et al., 2006; Liebert, Hänsch, & Heinze, 2006). For dextran, where this position is not available, reaction of OH groups with 3-azido-1,2-oxirane (Pahimanolis, Vesterinen, Rich, & Seppala, 2010) or the above mentioned carbonate ester function was used for decorating the polymer with azido groups with a DS of up to 0.20 (Geest et al., 2008). Nucleophilic addition to oxiranes has also been used for the less often applied introduction of the alkynyl groups to the dextran backbone for further coupling to 6-azido-6-deoxy-cyclodextrins (Nielsen, Wintgens, Amiel, Wimmer, & Larsen, 2010). By our approach employing etherification with alkynyl halides, the distance between the polymer backbone and recognition sites or linked functional groups can be easily tuned by varying the C-number of the alkynyl groups. The DS and the regioselectivity of the reaction can be controlled by the reaction conditions (Tahir et al., 2010), especially the amount of base. In contrast to esterification, etherification is kinetically controlled and proceeds with different regioselectivity. Thus, our approach differs markedly from other synthetic pathways reported in the literature. The higher stability of the linkage to the polysaccharide backbone will also be advantageous for e.g. biosensor applications or implant coating.

We now report on the preparation, characterization, and properties of various dextrans functionalized by 1,3-dipolar cycloaddition of azides to a well characterized *O*-pentynyl dextran.

2. Materials and methods

2.1. General

Dextran (Mw 500,000, from *Leuconostoc* sp.), DMSO, pyridine, acetic anhydride, dichloromethane, TFA, EDC, and streptavidin labeled with the fluorophor Atto 550 were purchased from Fluka, ethanol abs. from Merck, 5-chloro-1-pentyne, biotin and methyl lithium (1.6 M solution in diethylether) from Acros, 6-azido-*N*-Boc-hexylamine from Fluorochem (UK). *N*-Hydroxy succinimide (NHS) was purchased from Aldrich. For the surface binding studies of streptavidin to biotin, 430 μm n-doped Si(100) wafers, 1–50 Ω cm, were purchased from Siltronix, and cut into pieces of 8 mm × 8 mm. H_2SO_4 (96%), CMOS™, and H_2O_2 (30%) were purchased from J.T. Baker, HF etching mixture AF 87.5–12.5 VLSI Selectipur from BASF. All chemicals were used without any further purification or process except dextran which was dried before use.

2.2. Fluorimetry

Jasco Spectrofluorometer FP-6200 was used for fluorimetry. Biotinylated *O*-pentynyl dextran was treated with aqueous solution of labeled streptavidin and washed with water several times. After drying and dissolving in DMSO, fluorescence was recorded at 555 nm.

2.3. Ellipsometry

A DRE EL X-02C ellipsometer was used with software: EL X-1 2.0. λ = 632.80 nm, angle of incidence α = 70°, RI_{Si}: 3.8816, RI_{SiO_2}: 1.4571; RI applied for PyD and PyD-biotin: 1.56 (value reported for dextran films), RI applied for streptavidin-Atto 550: 1.47 (value reported for unlabeled streptavidin).

2.4. ^1H and ^{13}C NMR spectroscopy

NMR spectra were measured with a Bruker AMX 300 instrument (^1H: 300 MHz) or a Bruker AMX 400 (^1H: 400 MHz). Spectra were recorded in DMSO-d_6 or pyridine-d_5, or $CDCl_3$.Chemical shifts were calibrated to the residual proton and carbon resonances of the solvent: DMSO-d_6 (δ_H = 2.5, δ_C = 39.5 ppm), pyridine-d_5 (δ_H = 7.22, 7.58, 8.74; δ_C = 123.9, 135.9, 150.4 ppm), and $CDCl_3$ (δ_H = 7.25, δ_C = 77.0 ppm).

2.5. Elemental analysis

Thermoquest EA 1112 was used for elemental analysis. Data are the average of two measurements.

2.6. Infrared spectroscopy

Infrared spectra were recorded on Bruker Tensor 27 attenuated total reflectance infrared (ATR-IR) spectrometer.

2.7. Electrospray-ionization mass spectrometry (ESI-MS)

ESI-IT mass spectra (positive mode) were recorded on a HCT Ultra ETDII (Bruker Daltonics, Bremen, Germany), equipped with an ion trap. Spectra evaluation: Software Bruker Data Analysis Esquire-LC. Samples were introduced directly with a syringe at a flow of 100–200 μL h^{-1}. Nitrogen was used as dry gas (4 L min^{-1}, 325 °C) and as nebulizer gas (10 psi). Capillary: −3500 V, end plate offset: −500 V, nebulizer gas: N_2, 10 psi, capillary exit: 120 V, capillary exit offset: 90 V, skim 1: 30 V, skim 2: 10 V, trap drive: 50.4. Some of the ESI-MS spectra were recorded with HCT Ultra ETD-II, Bruker Daltronic GmbH, Bremen equipped with same software as for Esquire-LC. Instrument parameters so far deviating were set as: dry gas: 5 L min^{-1}, 300 °C, nebulizer gas: N_2, 5 psi, capillary exit: 181 V.

2.8. Sample preparation for the determination of the substituent distribution in dextran derivatives: methanolysis and trimethylsilylation

1.5 M methanol/HCl (900 μL) was added to 2 mg sample (PyD or click-products) in 1 mL V-Vial. It was heated at 90 °C for 2 h with

continuous stirring. After cooling to room temperature the reaction mixture was co-distilled with methanol (5×) under nitrogen to evaporate. For trimethylsilylation, 50 μL CH_2Cl_2, 10 μL pyridine, 50 μL *N,O*-bis-(trimethylsilyl)-trifluoroacetamide, and 10 μL chlorotrimethylsilane were added to the residue and heated at 100 °C for 1 h. The reaction mixture was diluted with CH_2Cl_2 (2 mL) and further analyzed by GLC. For ESI-MS, samples in MeOH without silylation were used.

2.9. Gas–liquid chromatography (GLC)

Carlo Erba GLC 6000 Vega Series instrument was used for GLC-FID analysis. Temperature program: 60 °C for 1 min; 20 °C min^{-1}–130 °C; 4 °C min^{-1}–290 °C and kept constant for 30 min. Data were recorded with a Merck Hitachi D 2500 Chromato-Integrator. Alternatively, a Shimadzu GC 2010 with split/splitless injector, FID and column (Phenomenex zebron ZB-5HT inferno, 5% phenyl and 95%-dimethylpolysiloxan, 30 m, ID 0.25 mm, film thickness 0.25 μm and 1.5 m retention gap (methyl deactivated) was used. H_2 (65 kPa) was used as carrier gas. Peaks were assigned by GCMS. For quantitative evaluation peak areas were corrected according to the effective-carbon-response (ECR) concept (Addison & Ackman, 1968; Scanlon & Willis, 1985); correction factors for PyD (Me-glc, *O*-Py/*O*-TMS): non-substituted ≡ 1.000, mono: 0.933; di: 0.874; tri: 0.823.

2.10. GCMS analysis

A Hewlett Packard 5890A gas chromatograph equipped with a 30 m column (ZBI, Phenomenex, 30 m × 0.32 mm ID, d_f = 0.25 μm) was used. Conditions: injector 250 °C, temperature program: 100 °C (3 min); 6 °C min^{-1}–310 °C (3 min), split ratio 1:20 or splitless mode, carrier gas: He (1.6 mL min^{-1}). The capillary column was directly coupled to a triple quadrupole mass spectrometer Finnigan TSQ 700. Transfer line was set at 250 °C, ion source temperature was set at 150 °C and ionization voltage at 70 eV.

2.11. O-Pentynyl dextrans (PyD)

O-Pentynyl dextran (**2**) was prepared with Li-dimsyl and 5-chloro-1-pentyne according to the procedure described previously (Tahir et al., 2010). Dextran (**1**), (Mw 500,000, from *Leuconostoc* sp.) was used and DS of product was 0.43. EA, ATR-IR and NMR data have been reported (Tahir et al., 2010). Monomer composition: s_i (mol%), s_0: 70.2%, s_2: 11.2%, s_3: 2.0%, s_4: 5.2%, s_{23}: 3.8%, s_{24}: 0.7%, s_{34}: 2.4%, s_{234}: 3.4%; c_0: 70.2, c_1: 18.4%, c_2: 7.0%, c_3: 3.4%; partial DS values x_i: x_2: 0.19, x_3: 0.12 x_4: 0.12, DS 0.43.

2.12. 4-Azidobutyric acid (**3**)

To 4-chlorobutyric acid (5.0 g, 4.08 mL, 40.8 mmol) in water (10 mL) NaN_3 (3.29 g, 50.6 mmol) was added. The reaction mixture was refluxed for 24 h before cooling to room temperature. Then 100 mL water was added and the product extracted with diethylether. The collected organic phases were washed with water and dried over $CaCl_2$. After evaporation of diethylether under reduced pressure the product was obtained as yellow oil (4.27 g, 33.0 mmol, 81%). TLC R_f: 0.38 (MeOH/*n*-hexane 1:1). ^{1}H NMR (300 MHz, $CDCl_3$): δ (ppm) = 1.92 (m, 2H, H-3), 2.50 (m, 2H, H-4), 3.38 (m, 2H, H-2) ppm. ^{13}C NMR (300 MHz, $CDCl_3$): δ = 24.13 (C-3), 30.93 (C-2), 50.63 (C-4), 178.09 (C-1).

2.13. 3-Azidopropane-1-thiol (4)

3-Chloropropan-1-thiol (700 mg, 616 μL, 6.3 mmol) was added to a mixture of H_2O/C_2H_5OH (10 mL, 2:1, v/v) followed by the addition of NaN_3 (796.8 mg, 12.2 mmol). The reaction mixture was stirred for 24 h at 110 °C before cooling down to room temperature, followed by addition of water (50 mL). The product was extracted with diethyl ether, collected organic phases were washed with H_2O and dried over $CaCl_2$. After evaporation of diethyl ether the product was obtained as yellow oil (553.7 mg, 4.72 mmol, 75%). TLC R_f: 0.60 (MeOH/*n*-hexane 3:1). ^{1}H NMR (300 MHz, $CDCl_3$): δ (ppm) = 1.86 (m, 2H, H-2), 3.48 (m, 2H, H-3), 3.72 (m, 2H, H-1). ^{13}C NMR (300 MHz, $CDCl_3$): δ (ppm) = 28.25 (C-1), 35.26 (C-2), 49.69 (C-3).

3-Azido-1-propanol (**5**) was prepared as described (Boyer, Liu, Bulmus, Davis, Barner-Kowollik, & Stenzel, 2008) while 2-azidoethylamine (**6**), *O*-biotinyl-*N*-hydroxysuccinimide (**7**) and biotin-(*N*-2-azidoethyl)amide (**8**) were prepared according to Mayer and Maier (2007). *O*-Acetyl-α-tocopheryl-azide (**9**) was a gift of Prof. Thomas Rosenau, University of Natural Resources and Applied Life Sciences, Department of Chemistry, Vienna, Austria (Adelwöhrer, Rosenau, Kloser, Mereiter, & Netscher, 2006), and *N*-Boc-1-amino-6-azidohexane (**10**) was commercially available.

2.14. Cycloaddition reactions of O-pent-4′-ynyl dextran (2, PyD) with functionalized azides (**3–10**)

In a typical procedure, PyD (**2**, DS 0.43, M(AGU) 190.5) was dissolved in DMSO/H_2O (4:1 v/v, 10–15 mL). After formation of a clear solution, the azide (see Table 1) followed by freshly prepared 1 M aq. solution of Na-L-ascorbate (20 mol% per alkynyl group), and $CuSO_4 \cdot 5H_2O$ (5 mol% per alkynyl group) was added. The reaction mixture was stirred at room temperature for 96 h. The product was purified by dialysis against dist. water and freeze-dried. Conversion of alkynyl groups into 1,2,3-triazole derivatives was calculated from EA, GLC (after methanolysis and trimethylsilylation) and ^{1}H NMR spectroscopy (if the product was soluble in an appropriate solvent).

2.14.1. Cycloaddition of 2-amino-ethylazide (**6**) to PyD (→**11**, PyD-2-NH_2)

EA: C 44.07%, H 6.5%, N 10.11%, C/H 6.78; corresponding to a conversion of 95%. GLC: residual DS_{Py}: 0.01, corresponding to a conversion of 98%. ATR-IR: $\tilde{\upsilon}$ [cm^{-1}] 3344, ν (O—H, s), 2925, 2883 ν (CH, CH_2, aliph., m), 1652 ν (C=C, v), 1519 ν (NH_2, m), 1436, 1352, 1280, δ (CH, m), 1148, 1102, 1014 ν (C—O).

2.14.2. Cycloaddition of 6-azido-N-Boc-hexylamine (**10**) to PyD (→**12**, PyD-6-NH-Boc)

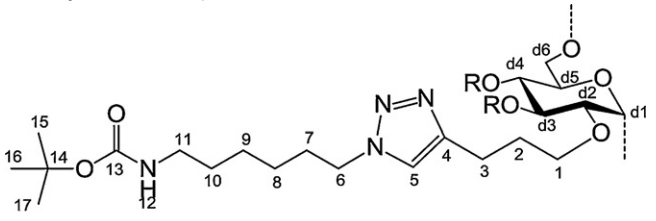

12

EA: C 51.47%, H 7.69%, N 7.41%, C/H 6.69, corresponding to 86% conversion. GLC: residual DS_{Py}: 0.10, corresponding to a conversion of 77%. ^{1}H NMR (400 MHz, DMSO-d_6): δ = 1.23 (m, 4H, H-8, 9), 1.36 (s, 9H, H-15, 16, 17), 1.77–2.89 (10H, H-2, -3, -7, -10, -11), 3.0–4.0 (glucose ring H, and H-1), 4.26 (2H, H-6), 4.69 and 4.85 (1H, H-d1), 6.72 (1H, H–12), 7.80 (s, 1H, H-5) ppm; estimated conversion: ca. 90%. ATR-IR: $\tilde{\upsilon}$ [cm^{-1}] 3351, ν (O—H, s), 2932, 2884 ν (CH, CH_2, aliph., m), 1691 ν (ROC=O), 1650 ν (C=C, v), 1524 ν (NH, m) 1455, 1365, 1237, δ (CH, m), 1156, 1104, 1015 ν (C—O).

Table 1
Overview of the performed cycloaddition reactions.

PyD, M(AGU) = 190 (**2**)			Azide				Product	Conversion of C≡CH (%)			
mg	AGU (mmol)	C≡CH (mmol)	No.	mg	mmol	Eq./C≡CH	Name	Yield (mg)	EA[a]	GLC[b]	NMR
201	1.05	0.45	**6**	94	1.10	2.4	PyD-2-NH_2 (**11**)	255	95	98	-
180	0.94	0.40	**10**	95	0.39	1.0	PyD-6-NH-Boc (**12**)	268	86	77	90
101	0.53	0.23	**5**	57	0.56	2.4	PyD-3-OH (**13**)	103	–[c]	98	>95
113	0.59	0.25	**3**	65	0.50	2.0	PyD-3-COOH (**14**)	175	83	85	78
114	0.60	0.26	**4**	66	0.56	2.2	PyD-3-SH (**15**)	186	–[c]	91	–
1120	5.88	2.53	**8**	717	2.29	0.9	PyD-Bio (**16**)	1420	75	63	75
142	0.75	0.32	**9**	334	0.65	2.0	PyD-Toc (**17**)	247	–[c]	56	–

[a] EA: elemental analysis.
[b] GLC: determined from residual DS(Py) after methanolysis and trimethylsilylation.
[c] Apparent conversion > 100%.

*2.14.3. Cycloaddition of 3-azido-1-propanol (**5**) to PyD (→**13**, PyD-3-OH)*

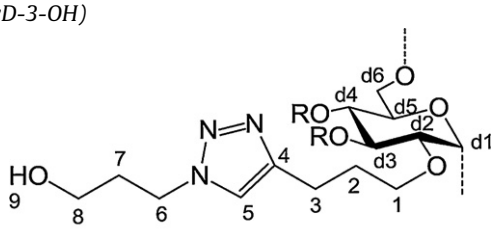

13

EA: C 43.95%, H 6.60%, N 10.05%, C/H 6.66. GLC: residual DS_{Py}: 0.01, corresponding to a conversion of 98%. ^{1}H NMR (400 MHz, DMSO-d_6): δ = 1.80–2.67 (6H, H-2, -3, -7), 3.0–4.0 (H-d2, 3, 4, 5, 6, 6′, H-8, H-1), 4.35 (s, 2H, H-6), 4.69 (s, 1H, H–d1), 7.82 (s, 1H, H–5) ppm; conversion: 100%. ATR-IR: $\tilde{\upsilon}$ [cm^{-1}] 3349, ν (O—H, s), 2926, 2880 ν (CH, CH_2, aliph., m), 1647 ν (C=C, v), 1446, 1348, 1281, δ (CH, m), 1146, 1104, 1010 ν (C—O).

*2.14.4. Cycloaddition of 4-azidobutyric acid (**3**) to PyD (→**14**, PyD-3-COOH)*

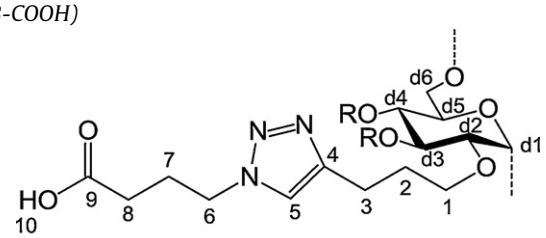

14

EA: C 44.76%, H 6.08%, N 6.32%, C/H 7.36, corresponding to a conversion of 83%; GLC: residual DS_{Py}: 0.07, corresponding to a conversion of 85%. ^{1}H NMR (400 MHz, DMSO-d_6): δ = 1.79–2.21 (6H, H-2, -3, -7), 2.67 (s, H, CH, residual C≡CH), 3.0–4.0: glucose ring H and 2H, H-1, 4.67 (H, H-d1), 4.92: OH. 7.83 (s, 1H, H-5) ppm; conversion: 78%.

ATR-IR: $\tilde{\upsilon}$ [cm^{-1}] 3375, ν (O—H, s), 2927, 2881 ν (CH, CH_2, aliph., m), 1712 ν (C=O, v), 1446, 1353, 1280, δ (CH, m), 1149, 1103, 1020 ν (C—O).

*2.14.5. Cycloaddition of 3-azido-1-propanethiol (**4**) to PyD (→**15** PyD-3-SH)*

EA: C 42.85%, H 6.05%, N 8.83%, S 9.08%, C/H 7.08, corresponding to an apparent conversion of 123%. GLC: residual DS_{Py}: 0.04, corresponding to a conversion of 91%.

ATR-IR: $\tilde{\upsilon}$ [cm^{-1}] 3371, ν (O—H, s), 2922, 2873 ν (CH, CH_2, aliph., m), 1645 ν (C=C, v), 1442, 1353, 1282, δ (CH, m), 1149, 1101, 1014 ν (C—O).

*2.14.6. Cycloaddition of biotin azide (**8**) to PyD (→**16**, PyD-Bio)*

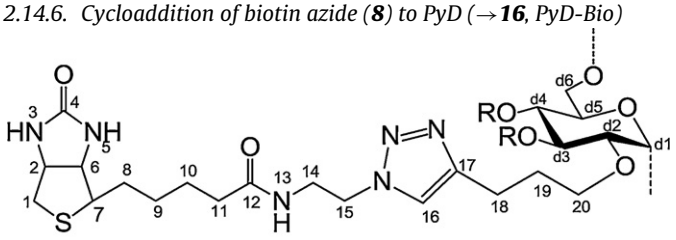

16

EA: C 48.78%, H 6.62%, N 9.32%, S 3.03%, C/H 7.37, corresponding to 75% conversion. GLC: residual DS_{Py}: 0.16, corresponding to 63% conversion. ^{1}H NMR (300 MHz, DMSO-d_6): δ = 1.26–2.24 (12H, H-8, -9, -10, -11, -18, -19), (2H, H-18), 2.60–4.00 (glucose ring H, H-20, H-1 and H-7), 4.15 (m, 1H, H-1), 4.35 (m, 1H, H-2), 4.50 (2H, H-15), 4.69 (H-d1), 6.39 (s, 1H, H-3), 6.44 (s, 1H, H-5), 7.80 (s, 1H, H-16), 7.96 (s, 1H, H-13) ppm; estimated conversion: 75%. ATR-IR: $\tilde{\upsilon}$ [cm^{-1}] 3347, ν (O—H, s), 2928, 2882 ν (CH, CH_2, aliph., m), 1647 ν (C=C, v), 1552 ν (NH, w) 1448, 1348, 1277, δ (CH, m), 1148, 1104, 1015 ν (C—O).

*2.14.7. Cycloaddition of O-acetyl- α-tocopherol azide (**9**) to PyD (→**17**, PyD-Toc)*

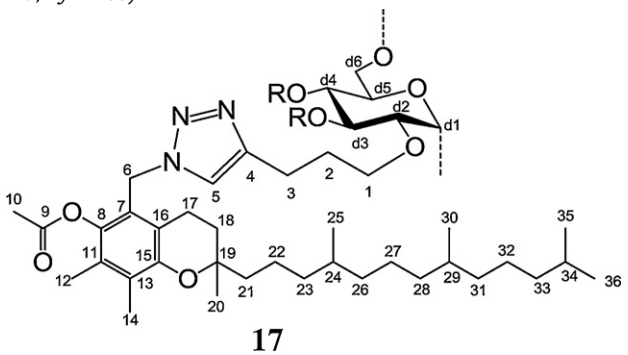

17

EA: C 61.29%, H 8.38%, N 4.54%, C/N 13.5, corresponding to an apparent conversion of 107%. GLC: residual DS_{Py}: 0.18, corresponding to 58% conversion. ^{1}H NMR (400 MHz, pyridine-d_5): δ = 0.89–1.90 (m, 33H, H-21 to H-36), 2.08–2.38 (8H, H-3, -12 and -14), 3.0–4.6 (glucose ring H, H-1), 4.7–5.3 (glucose OH), 7.75 (m, 1H, H-5) ppm. ^{13}C NMR (400 MHz, pyridine-d_5): δ = 12.38 (C-14), 13.24 (C-12), 19.85 (C-25, -30), 19.91 (C-22), 20.42 (C-10), 21.27 (C-17), 22.81 (C-35, -36), 23.86 (C-20), 25.10 (C-27, -32), 28.19 (C-34), 30.89 (C-18), 33.04 (C-14, -29), 37.66 (C-23, -26, -28, -31), 39.56 (C-21, -33), 46.49 (C-6), 75.87 (C-19), 118.74 (C-16), 128.37 (C-13), 126.90 (C-11), 141.99 (C-8), 169.72 (C-9) ppm. ATR-IR: $\tilde{\upsilon}$ [cm^{-1}] 3383, ν (O—H, s), 2950 ν (CH, arom., v), 2925, 2868 ν (CH, CH_2, aliph., m), 1641 ν (C=C, v), 1459, 1369, 1257, δ (CH, m), 1154, 1107, 1013 ν (C—O).

2.15. Binding studies of streptavidin-Atto 550 to PyD-Bio (**16**)

The Si wafers were cleaned with Piranha solution (96% H_2SO_4/30% H_2O_2 1:1) for 5 min at 100 °C. Native oxide layer was removed by immersion in HF etching mixture for 1 min at room temperature. Subsequently, the wafers were oxidized for 2 h at 800 °C in a muffle furnace, resulting in 12.3 ± 0.4 nm oxide layer as determined by ellipsometry. Silicon substrates were ultrasonic cleaned for 3 min in EtOH just before spin coating. – Solutions of PyD-Bio in DMSO and pyridine (1 and 3.3%), and for comparison a solution of PyD in DMSO was prepared. Solutions were spin-coated at 2000 rpm for 300 s, directly, after centrifugation for 15 min at 5000 rpm, and/or micro filtration. PyD-Bio and PyD-films were incubated in a 0.008% aq. solution of Atto 550-labeled streptavidin for 10 min, rinsed with water and dried in a stream of nitrogen. Thickness of dry films was measured by ellipsometry before and after incubation with streptavidin. All data and results are listed in Table 2. Furthermore, PyD and PyD-Bio coated surfaces were considered in a Leitz Ergolux microscope in the normal light mode before, and in fluorescence mode after incubation of films with in streptavidin-Atto 550.

2.16. Antioxidant activity

The TEAC (Trolox equivalent antixidant capacity) value was determined according to Re et al. (1999). Calibration was freshly performed with Trolox (6-hydroxy-2,5,7,8-tetramethylchroman-2-carboxylic acid) for each set of measurements. Reduction of absorbance of the ABTS-radical cation (2,2′-azino-bis(3-ethylbenzolthiazoline-6-sulfonic acid)) at 734 nm was measured after addition of the calibration standards or the sample. Samples were prepared by methanolysis of PyD-Toc (**17**) and for comparison by *O*-acetyl tocopherol azide **9**, to remove the acetyl protecting group, yielding the corresponding methyl glucosides of PyD-Toc (**17**). Mild methanolysis (0.1 M MeOH/HCl, 40 °C, 1 h) resulted only in partial deprotection. TEAC is expressed as equivalents to the Trolox-standard in mmol L^{-1}. PyD (**2**), PyD-2-NH_2 (**11**), and PyD-3-OH (**13**) were measured for comparison and showed all no activity.

3. Results and discussion

3.1. O-Pentynyl dextrans

The goal of our work was to employ a dextran derivative, well characterized with respect to the distribution of reactive substituents, as starting material for furnishing it in these predefined positions with a number of functional groups or signal molecules. In previous work, we have studied the formation of alkynyl dextrans with respect to the regioselectivity and efficiency of the reaction (Tahir et al., 2010). For this ongoing work, a pentynyl dextran (PyD, **2**) with a DS of 0.43 (average number of substituted OH/glc) was prepared in gram scale and characterized by elemental analysis, NMR spectroscopy, and monomer analysis. The portions of non-, mono-, di- and trisubstituted glucosyl residues were 71.0, 18.6, 7.0, and 3.4 mol%. Partial DS values at O-2, O-3, and O-4 were 0.19, 0.12, and 0.12, respectively. Small amounts of pentynylation at primary 6-OH of terminal glucosyl residues from side chains (7.5% branching at O-3) were also detected.

3.2. Functionalization of PyD by "click-reaction"

Our project on alkynyl polysaccharides compasses further functionalization of the terminal alkyne groups. Model studies with methyl 4,6-*O*-benzylidene-2,3-di-*O*-propargyl-α-D-glucoside and subsequently with starch (Tankam, Müller, et al., 2007) had shown that Mannich type aminations and 1,3-dipolar cycloaddition of azides ("click-reaction") are most appropriate for carbohydrates containing free OH beside alkynyl residues. Especially click reaction is tolerant against many common functional groups and solvents. To introduce amino, hydroxy, and other functionalities X, the pentynyl dextran was reacted with the corresponding alkyl azides (**3**–**6**, **8**) of the general formula N_3—$(CH_2)_n$X with different spacer lengths (n = 0, 2, 3 or 6; Scheme 1). Reactions were performed in DMSO/water (4:1) with $CuSO_4 \cdot 5H_2O$ and Na-L-ascorbate at room temperature for 4 days and products (**11**–**15**) were isolated by dialysis. Triazole formation could be recognized in the ^{1}H NMR spectra from the proton resonance of the triazole–CH at 7.8 ppm. Data are summarized in Table 1 (Section 2).

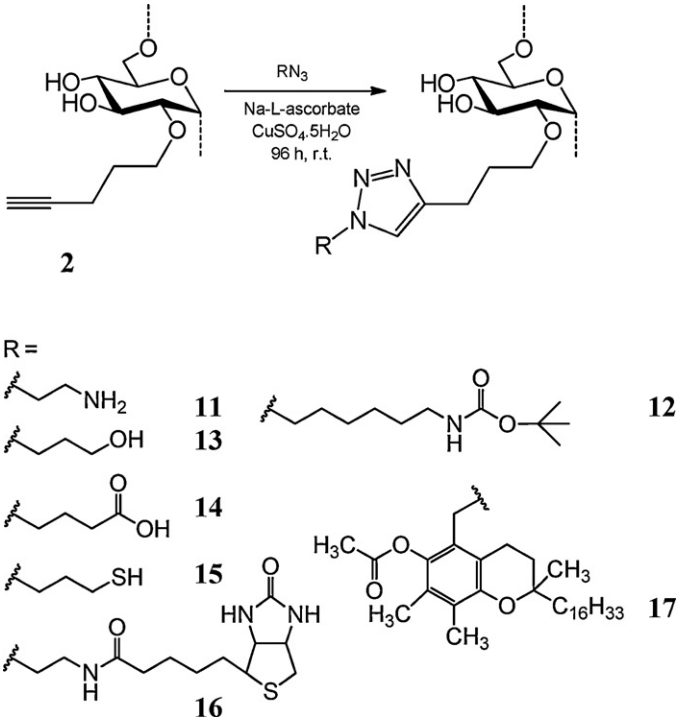

Scheme 1. [2+3]-Cycloaddition of various azides and *O*-pentynyl dextran (PyD, **2**).

Addition of 2-azidoethylamine (**6**) *to PyD*. The product from 1,3-dipolar cycloaddition of 2-aminoethyl azide (**6** to PyD (→PyD-2-NH_2, **11**) was purified by dialysis and subsequently freeze dried. Increase of weight compared to the starting material with DS_{Py} 0.43 corresponded to full conversion (apparent yield = 106%). From elemental analysis 10.11% nitrogen at a C/N ratio (w/w) of 4.36 was determined. Often, average DS in polymer analogous reactions is simply calculated from the portion of the characteristic element of a polysaccharide derivative (e.g. N, S, Si), but complete elemental analysis is rarely reported, and therefore it is unknown whether the ratio of elements is also in agreement with the overall composition calculated for a certain DS. Since polysaccharides and their still hydrophilic derivatives easily adsorb water and might have entrapped other minor compounds, which cannot easily be removed by dialysis or extraction, data must be corrected for moisture content and impurities. In case of amino compounds salt formation and complexation of metal ions must also be considered. Therefore, elemental analysis data did not allow simply calculating the $DS_{triazole}$ from the nitrogen content, and thus not the exact rate of conversion, since the ratios of C, H and N did not fit to one distinct pair of DS values for DS_{Py} and DS_{NH_2}. C/N ratio fast decreases with DS (Fig. 1a) from 14.36 at DS 0.1 to 3.34 at DS 0.7 and further more slowly to finally 1.93 for DS 3.0.

Given a certain DS_{Py}, for example 0.6, C/N ratio decreases from 33 at 10% conversion to 3.6 at complete transformation, at DS_{Py} 0.5

Table 2
Ellipsometric data and calculated film thickness of PyD (**2**) and PyD-Bio (**16**) coated on Silicon wafers, (a) prior and (b) after incubation with Atto-550 labeled streptavidin.

Entry	Sample	c/f	Δ (°)	Ψ (°)	Thickness (nm)
(a) Before streptavidin incubation					
1	PyD[a]	c	132.33 ± 0.44	13.66 ± 0.05	6.0 ± 0.3
2	PyD[a]	–	129.92 ± 3.86	13.95 ± 0.51	7.3 ± 2.2
3	PyD[b]	c	80.61 ± 1.61	30.19 ± 0.56	55.3 ± 2.9
4	PyD[b]	–	82.67 ± 6.58	32.64 ± 5.80	57.4 ± 14.4
5	PyD-biotin[a]	c	129.39 ± 0.94	14.06 ± 0.14	7.8 ± 0.6
6	PyD-biotin[a]	–	125.32 ± 3.07	14.06 ± 0.36	10.2 ± 1.7
7	PyD-biotin[a]	c	125.44 ± 0.41	14.57 ± 0.09	10.0 ± 0.3
8	PyD-biotin[a]	–	120.47 ± 1.30	14.60 ± 0.19	13.2 ± 0.8
9	PyD-biotin[a]	c, f	125.24 ± 0.58	13.91 ± 0.14	9.4 ± 0.6
10	PyD-biotin[b]	c	89.84 ± 0.84	24.95 ± 0.44	39.9 ± 1.2
11	PyD-biotin[b]	f	74.74 ± 4.15	27.49 ± 1.52	59.3 ± 5.8
12	PyD-biotin[b]	c, f	100.34 ± 2.94	20.22 ± 0.95	27.5 ± 3.0
(b) After streptavidin incubation of sample (x)					
13 (1)	PyD		138.22 ± 0.88	12.88 ± 0.09	<0
14 (2)	PyD		137.75 ± 2.24	12.90 ± 0.24	<0
15 (7)	PyD-biotin		105.39 ± 1.48	19.02 ± 0.50	15.1 ± 1.8
16 (8)	PyD-biotin		101.51 ± 1.18	19.39 ± 0.32	15.8 ± 2.0

All samples were dissolved in DMSO except 5 and 6 which were dissolved in pyridine. c: centrifuged, f: filtered.
[a] 1% solution.
[b] 3.3% solution.

from 37 to 4.1, and at DS_{Py} 0.4 from 43 to 4.7 (Fig. 1b). Thus the C/N ratio of 4.36 determined for PyD-2-NH_2 fits in a DS_{Py} range of 0.4–0.5 and in every case indicates a high degree of conversion of >90%. In the ATR-IR spectrum (see SI, Fig. 1) all vibrations referred to alkynes (3280, 2117, 635 cm^{-1}) have disappeared and a new absorption band at 1652 cm^{-1} has occurred for the triazole, thus confirming a very high conversion of the pentynyl residues. At 3100 cm^{-1}, also a new absorption is observed probably due to triazole C=C–H vibration. For mass spectrometric analysis, dextrans were depolymerized with MeOH/HCl, yielding the corresponding methyl glucoside derivatives. These were directly investigated by ESI-MS, and after trimethylsilylation submitted to GLC analysis. The gas chromatogram is shown in comparison with that from the precursor PyD in Fig. 2. Only traces of the *O*-pentynyl glucose derivatives are still visible, while a group of small peaks shifted to higher retention times might present triazole products, but could not unambiguously be identified. From the remaining pentynyl-DS of about 0.01, a conversion of 98% is calculated, confirming EA results.

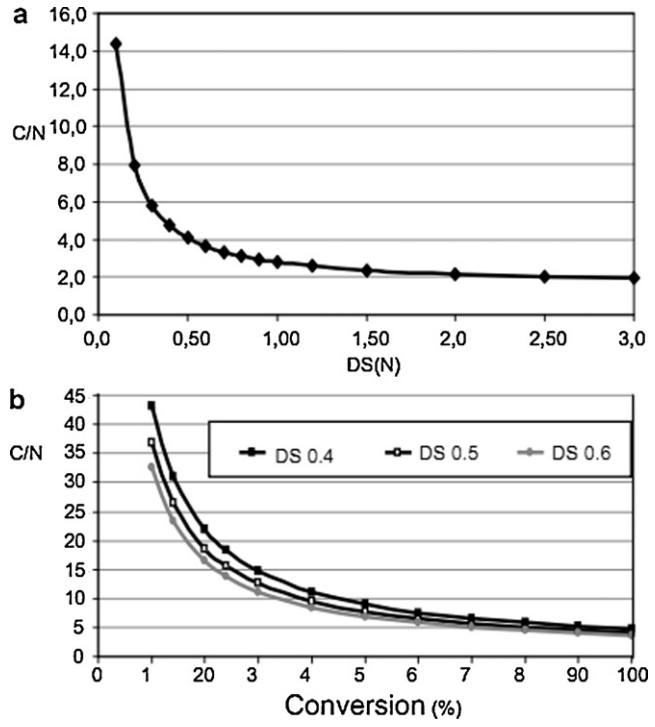

Fig. 1. (a) Change of C/N ratio with DS of *O*-pentynyl dextran (PyD) after complete conversion to aminoethyl triazole derivatives (11, PyD-2-NH_2); (b) change of C/N ratio with % conversion of pentynyl dextran in click reaction with 2-aminoethyl azide at a starting DS_{Py} of 0.40 (filled squares), 0.50 (open squares), and 0.6 (grey circles).

ESI-MS of PyD-2-NH_2 (**11**) was recorded after methanolysis (see SI, Fig. SI-2). *m/z* 347.3 is the main signal in the mass spectrum corresponding to $[M+H]^+$ of the mono-substituted methyl glucoside (**11a**). Second intensive signal at 361.4 with Δ = +14 compared to 347 is most probably due to methylation of triazole (**11a**-Me), since a product shifted by 14 units was observed for all triazole derivatives independently on their individual functionalities. A tiny peak at *m/z* 375 might be caused by additional *N*-methylation of the amino group (**11a**-Me_2) as a result of the methanolysis at elevated temperature (MeOH/HCl, 120 min at 90 °C), although this is commonly not observed. The relative intensities in MS do not reflect the molar proportions. Incompletely converted constituents bearing an additional pentynyl groups (**11b**, *m/z* 413) could also be detected. The signal of the sodiated non-substituted methyl glucoside at *m/z* 217 is nearly completely suppressed, although this component presents about 70 mol% of the sample. Beside the monosubstituted product (*m/z* 347.3), twofold (*m/z* 499.5) and even threefold triazolylpropyl-substituted product (*m/z* 651.5) could be detected. *m/z* 563.4 could not be assigned to a glucose derivative, but occurrence of *m/z* 715.5 (563 + 152; 152 = ΔM of substituent) indicates that it might bear various numbers of triazole groups. (The MS, a list and the structures of the discussed degradation products are summarized in the SI, Fig. SI-2, Table SI-3).

Addition of N-Boc-1-amino-6-azidohexane (**10**) *to PyD* (**2**). As an alternative approach of amino functionalization and for extending spacer length, protected *N*-Boc-1-amino-6-azidohexane (**10**) was employed. C/N ratio (N: 7.41%, C/N: 6.95) corresponded to 89% conversion (DS_{Py} 0.43, DS aminohexyltriazolyl: 0.38). The ATR-IR spectrum (see SI, Fig. SI-1) of protected PyD-6-NH-Boc (**12**) did not show any alkyne absorption, but C=O from the Boc-group.

The ^1H NMR spectrum (Fig. 3) shows several resolved signals of methylene groups of the pentynyl residue and the *N*-Boc-aminohexyltriazolyl residue, which are in the ratio of about 1:1 per H, confirming again a high conversion. The averaged integrals of the C–H resonance of the triazole at 7.82 ppm and the NH at 6.66 ppm

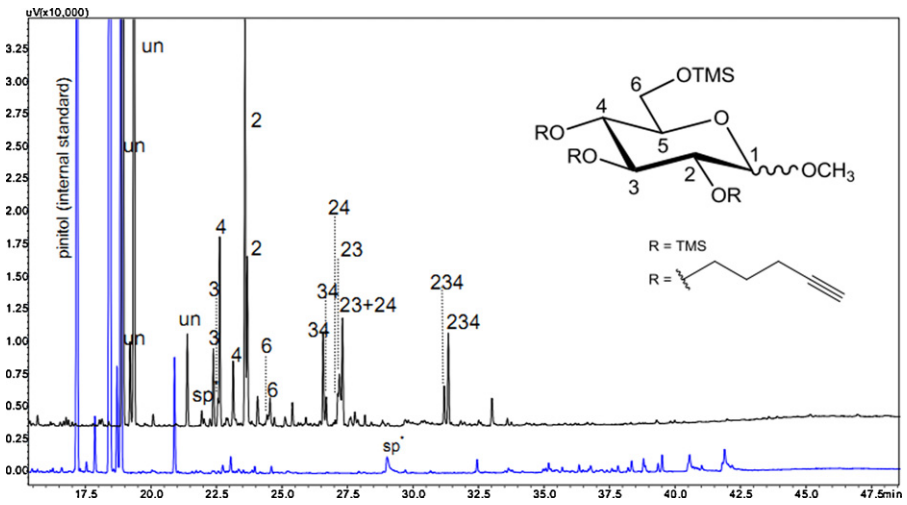

Fig. 2. Gas chromatograms of methyl glucoside derivatives obtained from PyD (2, upper trace), and from PyD-2-NH_2 (11, lower trace) after methanolysis and trimethylsilylation. Peaks are assigned according to the pentynyl substitution.

correspond to about 90% conversion, when referring to the NMR of PyD. Conversion estimated from GC analysis as described above was 77%. Purity of the *N*-protected compound was higher than for free amino derivative PyD-2-NH_2. Thus, amino-functionalized dextrans could be obtained from *O*-pentynyl dextran with a DS of 0.43 in high yield and at about 80–98% conversion.

ESI-MS of methanolyzed PyD-6-NH_2 (Fig. 4) showed mainly fully converted *O*-pentynyl glucosyl residues beside only partly converted di- and trisubstituted constituents (*m/z* 469.4, 535.5, 677.6). The *t*-butyloxycarbonyl protecting group had been removed during sample preparation for ESI-MS. Doubly charged (*m/z* 306) and signals with a mass shift of Δ14 are again detected due to triazole-methylation ($M+CH_3^+$ instead of $M+H^+$). Assignment of signals is summarized in SI, Table-SI-4.

Addition of 3-hydroxypropylazide (**5**) *to PyD* (**2**). Next, PyD was reacted with 3-hydroxypropyl-1-azide (**5**) under comparable conditions. In the ^{1}H NMR spectrum of PyD-3-OH (**13**) (see SI, Fig. SI-9) of the hydroxypropyl–triazolyl product, the triazole 5′-H can be clearly recognized as well as four of the six methylene groups at 1.75, 1.95, 2.70 and 4.30 ppm, while the two linked to oxygen are not resolved from the glucosyl ring protons. Only a small signal can still be observed at 2.17 ppm which corresponds to residual pentynyl groups. From the integrated signals a conversion of ≥95% is estimated. In the ATR-IR spectrum again all alkyne absorption bands had disappeared while those at 1652 and 3100 cm^{-1} occurred. Elemental analysis showed higher nitrogen content (10.05%) than expected for full conversion, while no residual azidopropanol was visible in the IR spectrum of the product. From remaining pentynyl derivatives in the gas chromatogram 98% conversion was calculated.

ESI-MS of PyD-3-OH (**13**) after methanolysis (see SI, Fig. SI-4 and Table SI-5) shows main signals at *m/z* 362.3, 529.5 and 696.52, representing mono-, di-, and tri-substituted functionalized glucosides, respectively. Again, “satellite”-signals followed the main signals with Δ (*m/z*) = +14. Weak signals with Δ (*m/z*) = +66, e.g. 362 + 66 = 428, 529 + 66 = 595 and 696 + 66 = 762, represent products containing one non-converted pentynyl group in mono-, di-, and tri-substituted trizaole product, respectively.

Addition of 4-azido butyric acid (**3**) *to PyD*. The click-reaction with 4-azido butyric acid could also be performed successfully

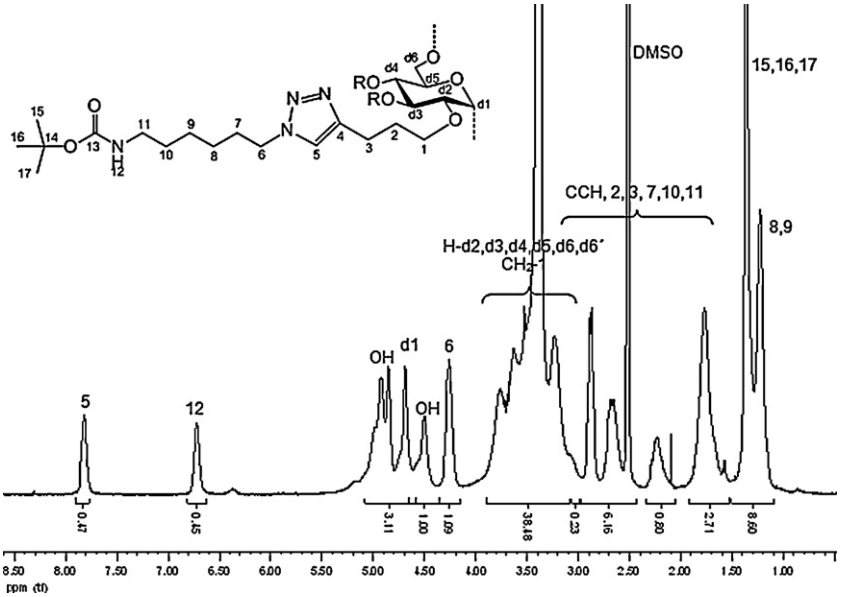

Fig. 3. ^{1}H NMR (300 MHz, DMSO-d_6) spectrum of *O*-(*N*-boc-aminohexyl-triazolyl)-propyl-dextran (PyD-6-NH-Boc, 12).

(→PyD-3-COOH, **14**). Conversion of pentynyl groups was estimated to be 83% (EA), 78% (NMR, see SI, Fig. SI-10), and 85% (GC, monomer analysis). Signals in the ESI-mass spectrum of the methanolyzed sample (COOH → COOMe) corresponded to the compounds obtained for the aminohexyl- (**11, 12**) and hydroxypropyl-triazolyl dextran (**13**), and thus confirmed an efficient transformation of alkynyl groups (see SI, Fig. SI-5, Table SI-6).

Addition of 3-azido-propanthiol (**4**) *to PyD*. Since a thiol group is of interest for the coating of plane or nanoparticle surfaces due to its high nucleophilicity and affinity to gold and silver, 3-azidopropan-1-thiol (**4**) was reacted with PyD to form PyD-3-SH (**15**). The IR-spectrum (see SI, Fig. SI-1) showed an absorption at 2100 cm^{-1}, which is partly caused by residual azide adsorbed to the product, but partly by disulfide bridge formation between linked and free thiol **4**, as was visible in ESI-MS after methanolysis. Consequently, conversion was overestimated from EA (apparent 123%), while GC monomer analysis corresponded to 93%. ESI-MS of PyD-3-SH after methanolysis (see SI, Fig. SI-6, Table SI-7) shows many peaks which do not correspond to any expected product of PyD or PyD-3-SH. Only a few peaks could be assigned, corresponding to non-substituted (*m/z* 217.1) and mono-substituted glucoside bearing al methyl group (M + CH_3^+, *m/z* 392.3). Since a signal with additional 14 u was detected (*m/z* 406.4), partly *S*-methylation is assumed to occur under methanolysis conditions (**15a**-Me_2); *m/z* 559.4 corresponds to formation of an intramolecular S—S bridge of a fully converted disubstituted glucose (**15d**), while *m/z* 752.4 is in agreement with compounds formed by S—S bridge between two different mono-substituted units (**15a**-ox-dimer).

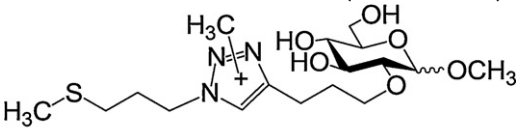

M: 406

15a-Me_2

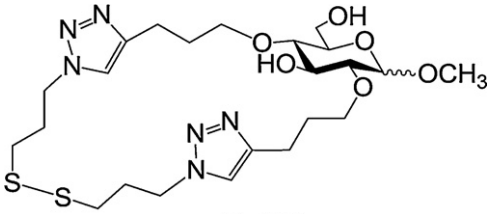

M: 558

15d-ox

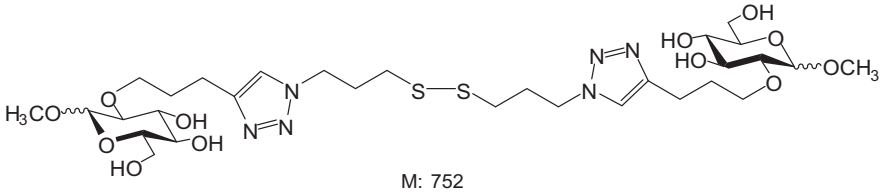

M: 752

15a-ox-dimer

Addition of N-(2′-azidoethyl)-biotinamide (**8**) *to PyD* (**2**). To introduce a tag for molecular recognition, biotin was linked to the 1-azido-2-aminoethan by amidation, and subsequently to dextran by cycloaddition to the C≡C- bond of PyD (see Scheme 1). Coupling of a homologous biotinyl azide probe to alkynyl monosaccharides, incorporated in cell glycans as reporting sugars, has been demonstrated by Hsu et al. (2007). The very strong and widely applicable biotin–streptavidin binding could be used for isolation of

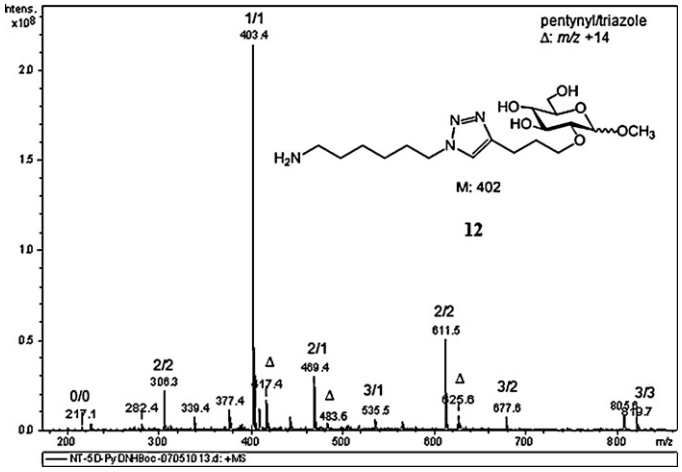

Fig. 4. ESI-MS of PyD-6-NH_2 (12) after methanolysis, peaks are assigned (*n*/*m*) according to the number of pyridine groups (*n*) and converted groups (*m*).

the labeled cells. For amidation, we followed the protocol of Mayer and Maier (2007), activating the biotin with EDC/NHS. Extending the reaction time improved yield to 82% compared to 51% reported by (Mayer & Maier, 2007), and 40% by a different approach reported by Hsu et al. (2007). The ATR-IR spectrum of PyD-Bio (**16**, see SI, Fig. SI-1) showed a significant decrease in alkynyl vibration but no complete disappearance as in the other click-reactions of PyD. ^{1}H NMR-spectrum (see SI, Fig.SI-11) also clearly indicates success of reaction, while some educt signals are still visible. Broadening of biotin signals gives evidence that it is linked to the polymer. Nearly all signals could be assigned by 2D-NMR and by comparison with the educt NMR spectra and literature data (Mayer & Maier, 2007). NH of amide and 5-H of triazole are observed at 7.96 and 7.80 ppm in a ratio of 1:1, the two NH of biotin are detected at 6.39 and 6.44 ppm. The methylene group from the former pentynyl residue now linked to the triazole (H-16) was not significantly shifted compared to the educt (see H-3′ in Fig. 4b). Therefore, this signal at 2.24 ppm can be taken as a measure for the reacted and unreacted pentynyl groups. The ratio of the averaged signal integrals of biotin-related protons to this methylene group correspond to a conversion of 75% ± 10%. Elemental analysis gave a higher N/S ratio than expected. While N/S (w/w) should be fixed in biotin at 2.62, a value of 3.08 was obtained. With respect to indications from NMR and IR spectra, and due to lower accuracy of sulfur determinations, calculation was based on the N content, corresponding to a conversion of 75% (DS_{Bio} 0.32) at a yield of 83% dextran. From GC analysis a transformation of 63% was calculated.

Beside the pattern of products discussed for the other click-products, a strong signal at *m/z* 259.2 in ESI-MS of PyD-Bio shows that biotin was partially released during methanolysis yielding aminoethyl triazole derivatives (**11a** and **11a**-Me, *m/z* 347.3/*m/z*

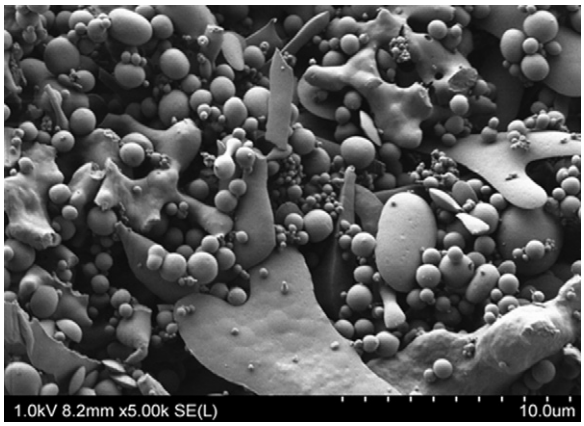

Fig. 5. SEM image of PyD-Bio (**16**) after dialysis from DMSO solution against water.

361.4). Mono-substituted methyl glucoside (**16a**, *m/z* 573.4) gave the strongest signal, while di-substituted product showed just a weak signal at *m/z* 725.5. (Spectrum and all peak assignments see SI, Fig. SI-7 and Table SI-8).

Addition of O-acetyl-tocopheryl azide (**9**) *to PyD* (**2**). As further functional group α-tocopherol was chosen for coupling to the polysaccharide due to its antioxidant activity. Almost equal (Arefiev, Domnina, Komarova, & Bilibin, 2000; Zielenski et al., 1993) or in case of ovalbumin coupling even enhanced antioxidant activity of dextran conjugates has been reported (Nakamura, Kato, & Kobayashi, 1992). Coupling of Trolox (6-hydroxy-2,5,7,8-tetramethylchroman-2-carboxylic acid), presenting the essential of the tocopherol structure, was performed by esterification (Zielenski et al., 1993). Antioxidants are widely applied as additives and cause problems with migration and contamination in the environment, especially when used in polymers. Linking to the polymer backbone is therefore of interest to immobilize the antioxidant and, increase its stability and maintain its activity. To stabilize the sensitive α-tocopherol the *O*-acetyl-protected tocopheryl azide **9** was employed (Adelwöhrer et al., 2006). The IR spectrum of PyD-Toc (Fig. SI-1) showed only weak residual alkyne absorption, but contamination with azide. Therefore, degree of conversion was overestimated from EA, while GLC data corresponded to 56%. Ester hydrolysis of tocopheryl acetate occurred during methanolysis, but in contrast to alkaline treatment, tocopherol is stable under acidic conditions. In the ESI-mass spectrum (see SI, Fig. SI-8, Table SI-9) deacetylated mono- (**17a**, *m/z* 733), di- (*m/z* 1270), and tri-substituted glucosides (*m/z* 1808) were detected along with some typical signals shifted by 66 units corresponding to unconverted alkynyl groups. (For ^{1}H NMR in pyridine-d_5 see SI, Fig. SI-12.)

The substituent pattern of all products is preset by the pentynylation step. Even if conversion is not complete, the functional group distribution could be calculated by statistics, assuming that in contrast to the first derivatization step, the reaction of the alkynyl groups is not position dependent but decoupled from the electronical and sterical effects of the polysaccharide backbone.

3.3. Properties of pentynyl dextran derivatives

Scanning electron micrographs of biotinylated PyD (PyD-Bio) showed interesting microstructure formation, including spherical, cylindrical and planar shapes (Fig. 5), similar to what has been observed for the precursor PyD (Tahir et al., 2010) even at the relatively low DS 0.43. It is assumed that this is due to the amphiphilic character of the material which is probably amplified by the strong heterogeneity of substituent distribution, as indicated on the monomeric (glucose) level by the outstanding deviation from a random distribution (Tahir et al., 2010).

The biotin–streptavidin system is widely used in reporter formates (probes) for DNA or protein detection, but also in glycan imaging as reported above (Hsu et al., 2007). The strong complex formation with streptavidin ($K_d = 10^{15}$) (Green, 1975), a tetrameric protein with four binding-sites, allows specific binding and amplification, e.g. in DNA-hybridization probes. Wenz and Liepold functionalized cellulose with biotin and showed their binding affinity to streptavidin (Wenz & Liepold, 2007). Therefore, biotin had been selected to provide dextran with these anchors for streptavidin mediated coupling or recognition processes.

Coupling with streptavidin was proved in dispersion and after immobilization on a silicon surface. PyD-Bio was stirred in an aqueous solution of streptavidin, labeled with a fluorophor (Atto 550). To prove that streptavidin was not unspecifically adsorbed on PyD, a control experiment was carried out with the latter. After incubation with streptavidin, both, PyD and PyD-Bio were washed thoroughly with water and dried. Fluorescence was recorded for solutions of both samples (Fig. 6). PyD-Bio showed strong fluorescence at 555 nm while PyD did not show any, confirming that streptavidin was specifically bound to biotin.

In a second experiment, biotin-dextran was spin-coated from DMSO or pyridine solution of various concentrations on silicon wafers. Surfaces were characterized by light microscopy, AFM and ellipsometry. Thicknesses of the layers were determined to be in the order of 10 nm from a 1% solution, depending on preparation of the PyD-Bio solution. After centrifugation, slightly thinner and better reproducible films were obtained, and measurements show lower standard deviation (entries 5, 7 and 9) than without (entries 6 and 8), indicating more uniform solutions. For details of the data, see Table 2. With 6.0 ± 0.3 nm the thickness of the PyD-film prepared under comparable conditions (entry 1) was lower than for the biotinylated product.

After incubation with streptavidin-Atto 550 and washing, strong fluorescence was observed by fluorescence microscopy, while the control experiment with PyD again confirmed the absence of unspecific adsorption also for the surface preparation (Fig. 7). The results were confirmed by ellipsometry as well (Table 2, entry 13–16).

Tocopherol is well known for its antioxidant activity. The TEAC (Trolox equivalent antioxidant capacity) test in the modification of Re et al. (1999). is based on the decolorization of the radical cation of 2,2′-azinobis-(3-ethylbenzothiazoline-6-sulfonic acid, $ABTS^{\bullet+}$), generated by oxidation with $K_2S_2O_8$. The method is calibrated with so called Trolox, presenting the basic tocopherol structure, and the antioxidant activity expressed relative to this standard [mmol] under the same conditions. Beside their health effects, antioxidants are important, e.g. to protect sensitive compounds like unsaturated fatty acids in food and cosmetics, but also as widely used additives in polymeric materials, what causes significant pollution problems. Chitosan nanoparticles have been grafted with eugenol and carvacrol derived aldehydes (Chen, Shi, Neoh, & Kang, 2009). Phenolic antioxidants have also been coupled to synthetic polymers (Yamaguchi, Itoh, Ishikawa, & Kusuda, 1993) and polysaccharides (Arefiev et al., 2000), and dextran hase been esterified with Trolox (Zielenski et al., 1993). In our case, *O*-acetyl-tocopherylazide was chosen as a potential antioxidant for the click reactions to the PyD of DS 0.43.

The *O*-acetyl-tocopheryl residue linked to the dextran had first to be deprotected due to the key role of the phenolic OH for the radical scavenging property. When this deacetylation was performed with KOH in ethanol, antioxidant activity was strongly reduced not only for the tocopheryl–dextran, but also for the tocopheryl azide itself due to the oxidation, and dimerization initiated by the phenolate anion (Adelwöhrer et al., 2006). When acetate hydrolysis was

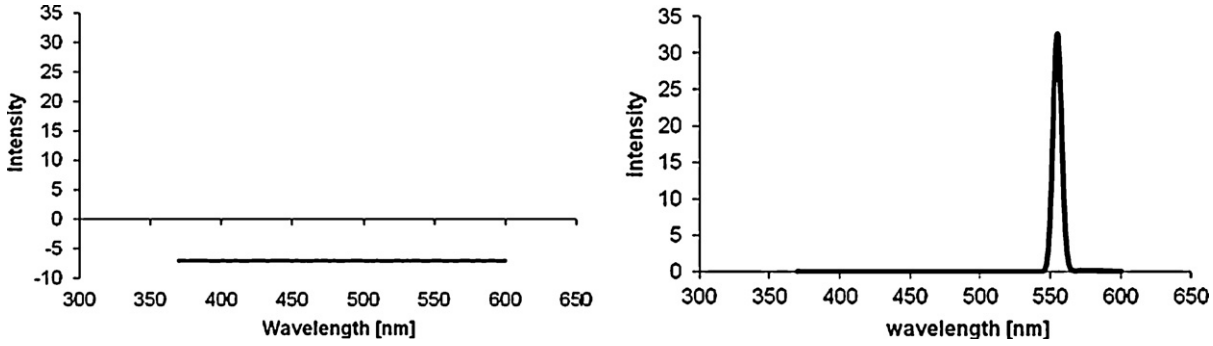

Fig. 6. Fluorescence of PyD (left) and PyD-biotin (right) treated with labeled streptavidin.

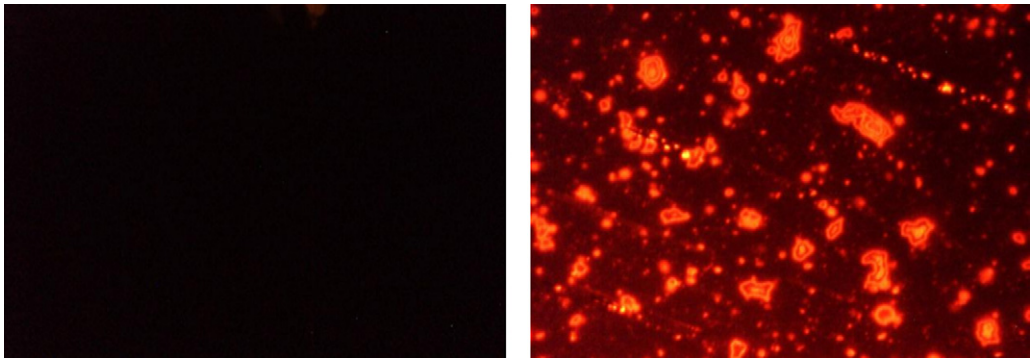

Fig. 7. Fluorescence of Streptavidin-Atto-550 linked to a PyD-Bio-layer on a silicon support. Left: control with PyD (**2**), right: PyD-Bio (**16**) prepared by spin coating without centrifugation of the sample solution (for additional information see SI).

carried out under acidic conditions with MeOH/HCl, full activity was retained (referred to the tocopherol content, estimated DS_{Toc} 0.24 for 56% conversion) corresponding to the structurally similar Trolox standard (1 mmol L^{-1} TEAC) for the resulting methyl glucoside derivatives, showing no loss of activity compared to the free tocopheryl azide. In contrast, control experiments PyD, PyD-2-NH_2 and PyD-3-OH showed no activity at all.

4. Conclusion

O-Pent-4′-ynyl dextran with DS 0.43 has been used as precursor for the preparation of various functionalized dextrans. Aminoalkyl, hydroxyalkyl, carboxyalkyl, thioalkyl, biotinyl-, and tocopheryl triazole derivatives were obtained by [2+3]-cycloaddition with the corresponding azides. Conversions of terminal alkyne groups were between approx. 60% and nearly 100%. Only the thiol showed some side products like disulfide formation with residual free or bound azidopropanthiol. Products were characterized by elemental analysis, ATR-IR and ^{1}H NMR spectroscopy, and GLC and ESI-MS after depolymerization to methyl glucosides. Biotinylated dextran formed microstructures by dialysis from solution against water as shown by SEM. Due to the heterogeneity of substituent distribution observed for alkynyl dextrans the compounds have amphiphilic properties, supporting microparticle formation by phase separation. It was demonstrated that PyD-Bio in dispersion as well as spin-coated on a surface, binds streptavidin while pentynyl dextran used for control did not. Tocopherol-functionalized methyl glucosides obtained from the corresponding dextran PyD-toc by methanolysis showed no loss in antioxidant capacity compared to free tocopherol. The concept allows variation of both alkynyl and azidoalkyl spacer length and the introduction of a wide range of functionalities, bioactive molecules and recognition sited with high yield. The substitution pattern can be determined in detail for the starting pentynyl dextran, which affects the pattern of all final functionalized products.

Acknowledgments

This work was supported by the Deutsche Forschungsgemeinschaft, DFG-Mi398/9-1. Financial support of M.N.T. by the DAAD is gratefully acknowledged. We thank Prof. Thomas Rosenau, Vienna, for the gift of tocopherol azide, and Dr. Silke Hillebrand, Lars Henneicke, Daniela Butschbach, and Christian Bork for the TEAC test measurements.

Appendix A. Supplementary data

Supplementary data associated with this article can be found, in the online version, at doi:10.1016/j.carbpol.2011.11.082.

References

Addison, R. F., & Ackman, R. G. (1968). Flame ionization detector molar responses for methyl esters of some polyfunctional metabolic acids. *Journal of Gas Chromatography*, *6*, 135–138.

Adelwöhrer, C., Rosenau, T., Kloser, E., Mereiter, K., & Netscher, T. (2006). Synthesis of 5a-α-tocopheryl azide and its reaction to 1-(5a-α-tocopheryl)-1,2,3-triazols by [2+3]-cycloaddition. *European Journal of Organic Chemistry*, *2006*(9), 2081–2086.

Arefiev, D. V., Domnina, N. S., Komarova, E. A., & Bilibin, A. Y. (2000). Sterically hindered phenol–dextran conjugates: Radical scavenging activity in water and water–organic media. *European Polymer Journal*, *36*(4), 857–860.

Aumelas, A., Serrero, A., Durand, A., Dellacherie, E., & Leonard, M. (2007). Nanoparticles of hydrophobically modified dextrans as potential drug carrier systems. *Colloids and Surfaces B: Biointerfaces*, *59*(1), 74–80.

Bertoldo, M., Nazzi, S., Zampano, G., & Ciardelli, F. (2011). Synthesis and photochromic response of a new precisely functionalized chitosan with "clicked" spiropyran. *Carbohydrate Polymers*, *85*(2), 401–407.

Bock, V. D., Heimstra, H., & Maarseveen, J. H. V. (2006). Cu-catalyzed alkyne-azide "Click" cycloadditions from a mechanistic and synthetic prospective. *European Journal of Organic Chemistry*, 51–68.

Boyer, C., Liu, J., Bulmus, V., Davis, T. P., Barner-Kowollik, C., & Stenzel, M. H. (2008). Direct synthesis of well-defined heterotelechelic polymers for bioconjugations. *Macromolecules*, *41*(15), 5641–5650.

Chen, F., Shi, Z., Neoh, K. G., & Kang, E. T. (2009). Antioxidant and antibacterial activities of eugenol and carvacrol-grafted chitosan nanoparticles. *Biotechnology and Bioengineering*, *104*(1), 30–39.

Dorner, S., & Westermann, B. (2005). A short route for the synthesis of "sweet" macrocycles via a click-dimerization–ring-closing metathesis approach. *Chemical Communications*, (22), 2852–2854.

Durand, A., Marie, E., Rotureau, E., Leonard, M., & Dellacherie, E. (2004). Amphiphilic polysaccharides: Useful tools for the preparation of nanoparticles with controlled surface characteristics. *Langmuir*, *20*(16), 6956–6963.

Geest, B. G. D., Camp, W. V., Prez, F. E. D., Smedt, S. C. D., Demeester, J., & Hennink, W. E. (2008). Biodegradable microcapsules designed via 'click' chemistry. *Chemical Communications*, (2), 190–192.

Green, N. M. (1975). Avidin. *Advances in Protein Chemistry*, *29*, 85–133.

Hasegawa, T., Umeda, M., Numata, M., Li, C., Bae, A.-H., Fujisawa, T., et al. (2006). Click chemistry" on polysaccharides: A convenient, general, and monitorable approach to develop (1->3)-β-D-glucans with various functional appendages. *Carbohydrate Research*, *341*, 35–40.

Heinze, T., Liebert, T., Heublein, B., & Hornig, S. (2006). Functional polymers based on dextran. *Advances in Polymer Sciences*, *205*, 199–291.

Hennink, W. E., De Geest, B. G., Van Camp, G., & Du Prez, F. (2009). *Biodegradable hydrogels based on click chemistry*. European Patent Application EP2090592-Al.

Hornig, S., & Heinze, T. (2007). Nanoscale structures of dextran esters. *Carbohydrate Polymers*, *68*, 280–286.

Hornig, S., Heinze, T., Hesse, S., & Liebert, T. (2005). Novel nano particles based on dextran esters with unsaturated moieties. *Macromolecular Rapid Communications*, *26*, 1908–1912.

Hornig, S., Liebert, T., & Heinze, T. (2007). Structure design of multifunctional furate and pyroglutamate esters of dextran by polymer-analogous reactions. *Macromolecular Bioscience*, *7*, 297–306.

Hsu, T.-L., Hanson, S. R., Kishikawa, K., Wang, S.-K., Sawa, M., & Wong, C.-H. (2007). Alkynyl sugar analogs for the labeling and visualization of glycoconjugates in cells. *Proceedings of the National Academy of Sciences*, *104*(8), 2614–2619.

Kolb, H. C., Finn, M. G., & Sharpless, K. B. (2001). Click chemistry: Diverse chemical function from a few good reactions. *Angewandte Chemie-International Edition*, *40*, 2004–2021.

Liebert, T., Hänsch, C., & Heinze, T. (2006). Click chemistry with polysaccharides. *Macromolecular Rapid Communications*, *27*(3), 208–213.

Liebert, T., Hornig, S., Hesse, S., & Heinze, T. (2005). Nanoparticles on the basis of highly functionalized dextrans. *Journal of the American Chemical Society*, *127*(30), 10484–10485.

Mayer, T., & Maier, M. E. (2007). Design and synthesis of a tag-free chemical probe for photoaffinity labeling. *European Journal of Organic Chemistry*, *2007*(28), 4711–4720.

Mischnick, P., & Momcilovic, D. (2010). Chemical Structure Analysis of Starch and Cellulose Derivatives. *Advances in Carbohydrate Chemistry and Biochemistry*, *64*, 117–210.

Nakamura, S., Kato, A., & Kobayashi, K. (1992). Enhanced antioxidative effect of ovalbumin due to covalent binding of polysaccharides. *Journal of Agricultural and Food Chemistry*, *40*(11), 2033–2037.

Nielsen, T. T., Wintgens, V. r., Amiel, C., Wimmer, R., & Larsen, K. L. (2010). Facile synthesis of β-cyclodextrin–dextran polymers by "Click" chemistry. *Biomacromolecules*, *11*(7), 1710–1715.

Pahimanolis, N., Vesterinen, A.-H., Rich, J., & Seppala, J. (2010). Modification of dextran using click-chemistry approach in aqueous media. *Carbohydrate Polymers*, *82*(1), 78–82.

Re, R., Pellegrini, N., Proteggente, A., Pannala, A., Yang, M., & Rice-Evans, C. (1999). Antioxidant activity applying an improved ABTS radical cation decolorization assay. *Free Radical Biology and Medicine*, *26*(9–10), 1231–1237.

Rotureau, E., Leonard, M., Dellacherie, E., & Durand, A. (2004). Amphiphilic derivatives of dextran: Adsorption at air/water and oil/water interfaces. *Journal of Colloid and Interface Science*, *279*(1), 68–77.

Scanlon, J. T., & Willis, D. E. (1985). Calculation of flame ionization detector relative response factors using the effective carbon number concept. *Journal of Chromatographic Science*, *23*, 333–340.

Tahir, M. N., Bork, C., Risberg, A., Horst, J. C., Komoß, C., Vollmer, A., & Mischnick, P. (2010). Alkynyl ethers of glucans: substituent distribution in propagyl-, pentynyl- and hexynyldextrans and -amyloses and support for silver nanoparticle formation. *Macromolecular Chemistry and Physics*, *211*, 1648–1662.

Tankam, P. F., Mischnick, P., Hopf, H., & Jones, P. G. (2007). Modification of methyl *O*-propargyl-D-glucosides: Model studies for the synthesis of alkynyl based functional polysaccharides. *Carbohydrate Research*, *342*, 2031–2048.

Tankam, P. F., Müller, R., Mischnick, P., & Hopf, H. (2007). Alkynyl polysaccharides: synthesis of propargyl potato starch followed by subsequent derivatization. *Carbohydrate Research*, *342*, 2049–2060.

Tornoe, C. W., Christensen, C., & Meldal, M. (2002). Peptidotriazoles on solid phase: [1,2,3]-Triazoles by regiospecific copper(I)-catalyzed 1,3-dipolar cycloadditions of terminal alkynes to azides. *Journal of Organic Chemistry*, *67*(9), 3057–3064.

Wenz, G., & Liepold, P. (2007). Self-assembly of biotin and thio-functionalized carboxymethyl celluloses on gold and molecular recognition of streptavidin detected by surface plasmon resonance. *Cellulose*, *14*(2), 89–98.

Wilkinson, B. L., Bornaghi, L. F., Poulsen, S.-A., & Houston, T. A. (2006). Syntheric utility of glycosyl triazoles in carbohydrate chemistry. *Tetrahedron*, *62*, 8115–8125.

Yamaguchi, H., Itoh, M., Ishikawa, H., & Kusuda, K. (1993). Antioxidant activity of polymers bearing hindered phenolic groups. *Journal of Macromolecular Science Pure and Applied Chemistry*, *A30*, 287–292.

Zielenski, J., Wu, T. W., Fung, K. P., Zeng, L. H., Li, R. K., Mickle, D. A. G., & Wu, J. (1993). Chemical syntheses of Trolox conjugates which protect human ventricular myocytes against in situ-generated oxyradicals. *European Journal of Pharmacology – Environmental Toxicology and Pharmacology*, *248*, 313–318.